On the threshold of flow in a tight natural rock

On the threshold of flow in a tight natural rock

P. G. Meredith,[1] I. G. Main,[2] O. C. Clint,[1] and L. Li[2]

Received 14 December 2011; revised 19 January 2012; accepted 19 January 2012; published 25 February 2012.

[1] The behaviour of hydraulically 'tight' barrier rocks is a key determinant of the long-term integrity of potential underground storage sites for the waste products from low-carbon emission energy production technologies (including nuclear waste and CO_2 captured from fossil fuels). Here we isolate the relationship between crack-induced permeability and porosity using an initially crack-free natural crystalline material. We vary secondary porosity from an initial value of zero, and demonstrate that the bulk permeability K varies with total connected porosity Φ above the percolation threshold Φ_c as $K = K_0(\Phi - \Phi_c)^n$, where $n = 3.8 \pm 0.4$, i.e., similar to results obtained for higher porosity rocks, indicating universality of this scaling law. Close to the percolation threshold a modest change in total porosity from 1% to 5% or so results in a massive change in permeability of 7 orders of magnitude or more. The results are consistent with a continuum percolation model that reflects the microstructure of the pore/induced microcrack network in the natural material. **Citation:** Meredith, P. G., I. G. Main, O. C. Clint, and L. Li (2012), On the threshold of flow in a tight natural rock, *Geophys. Res. Lett.*, *39*, L04307, doi:10.1029/2011GL050649.

1. Introduction

[2] Cracks and fractures exert a key role in determining fluid permeability at depth, notably in otherwise 'tight' rocks that may be used as seals for the subsurface storage of carbon dioxide or nuclear waste products associated with the mitigation of future climate change [*Intergovernmental Panel on Climate Change*, 2007; *Hopkin*, 2007]. To date it has not been possible to test suggested relationships for crack-induced porosity and permeability in very tight rocks. Almost all surface rocks contain natural fractures induced by the stresses that brought them there, making it difficult to make measurements at the lowest porosities relevant for deep underground storage, where such cracks may have yet to form. Similarly core samples obtained from depth in boreholes are also affected by drilling stresses. This makes it hard to unravel the relative contribution of primary porosity (due to the processes that initially formed the rock) and secondary induced microcracks formed at depth. In fact it is extremely rare to find a natural crystalline rock with no primary porosity to use as a control sample to make this comparison. One example is Frederick diabase, previously used to quantify the effect of pressure on the electrical resistivity of water-saturated crystalline rocks [*Brace et al.*, 1965]. Here we use an extremely rare type of silica-unsaturated, alkali-rich microgranite quarried from the island of Ailsa Craig (Figure 1), known by the quarryman's term Blue Home, which also has no detectable microcracks [*Harrison et al.*, 1987]. Its 'flawless' nature and isotropic properties make it the material of choice for the running surface of stones used in the Olympic winter sport of curling (Figure 2), due to its long-term strength and stability on ice rinks subjected to freeze-thaw weathering.

[3] Starting with this material, we deliberately induce crack porosity using thermal cracking and interpret the resulting permeability evolution using microstructural characterisation, as by *Fredrich and Wong* [1986] and *Darot et al.* [1992]. We confirm the relation between the measured porosity (of the connected network of pore space) and the effective bulk permeability inferred from Darcy's law conforms to a simple universal model for crack-induced permeability both near and well above the percolation threshold. The model and observed permeability is very sensitive to extremely small changes in microcrack density just above the percolation threshold.

2. Theory

[4] The aim of the experiments was to test the hypothesis that the porosity-permeability relation has the universal form expected for a system near the percolation threshold [*Wong et al.*, 1984; *Guèguen and Dienes*, 1989; *Mavko and Nur*, 1997; *Berkowitz and Balberg*, 1992, 1993; *Feng et al.*, 1987; *Stauffer and Aharony*, 1994; *Guèguen and Palciauskas*, 1994]:

$$K = K_0(\Phi - \Phi_c)^n, \tag{1}$$

where K is the permeability (in m^2), Φ is the total porosity (in %), Φ_c is the porosity at the percolation threshold for fluid flow across the sample, K_0 is a characteristic permeability when $\Phi - \Phi_c = 1\%$, and n is a critical exponent. This relation has been suggested on theoretical grounds based on percolation theory [*Berkowitz and Balberg*, 1992, 1993; *Feng et al.*, 1987], from pore network modelling [*Stauffer and Aharony*, 1994; *Zhu et al.*, 1995] and from empirical observation [*Zhang et al.*, 1994; *Mavko and Nur*, 1997]. Previous attempts to fit a simple power law, $K \sim \Phi^n$, to data for hot-pressed calcite in the range 4%–20% requires a sharp increase in n at a cross-over porosity of ~13% [*Zhu et al.*, 1995; *Bernabe et al.*, 1982], consistent with (1). For sandstones of porosity in the range 6%–25% a relation of the form (1) holds with n fixed at the integer value 3, the latter to retain consistency with the Kozeny-Carman relation at high porosity [*Mavko and Nur*, 1997]. For overlapping spherical pores, Monte-Carlo simulations give $n \approx 2.3$ [*Mavko and Nur*, 1997].

[5] For the inverse case of overlapping solid spheres, i.e., the 'Swiss cheese' model of *Berkowitz and Balberg* [1993, Figure 1], porosity is created in the gaps. Porosity is bimodal in this model, concentrated in open pores connected (or not)

[1]Department of Earth Sciences, University College London, London, UK.
[2]School of Geosciences, University of Edinburgh, Grant Institute, Edinburgh, UK.

0094-8276/12/2011GL050649

Figure 1. Ailsa Craig Island, viewed from the South. Note the steep slopes, indicating strong resistance to weathering, and the strong pattern of vertically-aligned joints on the cliff face. Photo by Davie Law: http://www.maybole.org/photogallery/ailsacraig/ailsacraig2.htm.

by slightly open (or completely closed) bottlenecks. Permeability is then more sensitive to porosity, so that $n \approx 4.5$ [*Berkowitz and Balberg*, 1993]. This model has previously been applied successfully to explain the nature of porosity and permeability evolution near the percolation threshold during hot isostatic pressing of calcite aggregates [*Zhang et al.*, 1994]. In this model connected bottlenecks form a network representing a set of Voronoi cells [*Berkowitz and Balberg*, 1993; their Figure 3], directly analogous to those which develop in crystallisation from a melt, and to the networks shown at high crack density in the photo-micrographs of Figure 3. Most cells formed by the fractures follow the original grain boundaries, but a few are intra-granular, hence reducing the co-ordination number of the original grain boundaries. With this caveat, the attributes of the microstructure of Ailsa Craig micro-granite then closely resemble those of the conceptual 'Swiss cheese' model: open pores (altered micro-phenocrysts) connected (or not) by narrow 'bottlenecks' in the form of slightly open cracks (or tight grain boundaries).

3. Materials and Methods

[6] The photo-micrograph shown in Figure 3 (top left) confirms that Ailsa Craig microgranite is both isotropic and crack-free. Using this starting material, we progressively introduced isotropic crack damage in a controlled and measurable manner by thermal stressing to different temperatures in the range 20–800°C, and studied how fluid permeability evolved near the percolation threshold, where previously isolated cracks nucleate and begin to link together to provide permeable pathways for fluid flow (Figures 3 (top right), 3 (bottom left), and 3 (bottom right)).

[7] Measurement of very low permeability presents a significant challenge. Here we use a method based on high-accuracy measurement of fluid flow volume both in and out of a sample under conditions of steady-state flow at the sample boundaries, [*Jones and Meredith*, 1998]. In this permeameter two separate pressure intensifiers are used (an upstream one and a downstream one) providing an independent verification of the inflow and outflow rate and whether these have achieved steady state. Only if these match do we accept the measurement as valid. The experiments were conducted in a temperature controlled laboratory inside a thick-walled steel pressure vessel with a high thermal capacity. These both act to minimise temperature fluctuations and any effect on the measured pressures and flow rates. The method has been used routinely and successfully to measure nano-Darcy permeability and below in a range of tight rocks [e.g., *Jones and Meredith*, 1998; *Nara et al.*, 2011]. Here the longest single steady-state flow measurement at the lowest permeability took 15 days, and the system was stable over this whole period. The effective bulk permeability is then calculated from the pressure drop and the steady-state flow rates at the upstream and downstream reservoirs, using the standard Darcy equation.

[8] The connected porosity of the starting material was determined using high-pressure gas porosimetry at Aberdeen University, Scotland and Sandia National Laboratory, New Mexico. After coring, the samples were oven dried prior to heat treatment, to ensure that any water retained in the sample after coring and grinding would not boil during heating and cause excess cracking. Samples were dried at 50°C, i.e., lower than the onset temperature of thermal cracking in this material at 75–80°C. A suite of samples was thermally-stressed to different ultimate temperatures [*Darot et al.*, 1992] and then cooled to induce a controlled range of crack porosities. To achieve this sample temperature was increased by 1°C per minute at ambient pressure, and then maintained at the pre-determined plateau temperature for 1 hour before a controlled temperature reduction, also at 1°C/min, was initiated. This rate results in a negligible temperature gradient across the sample and precluded any thermal shocking during heating or cooling [*Glover et al.*, 1995].

[9] The resulting samples, 38.1 mm in diameter by 40 mm long, were then jacketed in nitrile rubber jackets and placed in a conventional hydrostatic pressure vessel at room temperature. A confining pressure of 20 MPa was first applied, and pressurized pore fluid was then introduced using upstream and downstream reservoirs controlled using a dual servo-controlled fluid intensifier system [*Benson et al.*,

Figure 2. Photograph of a curling stone formed from Ailsa Craig Blue Hone (diameter 29 cm).

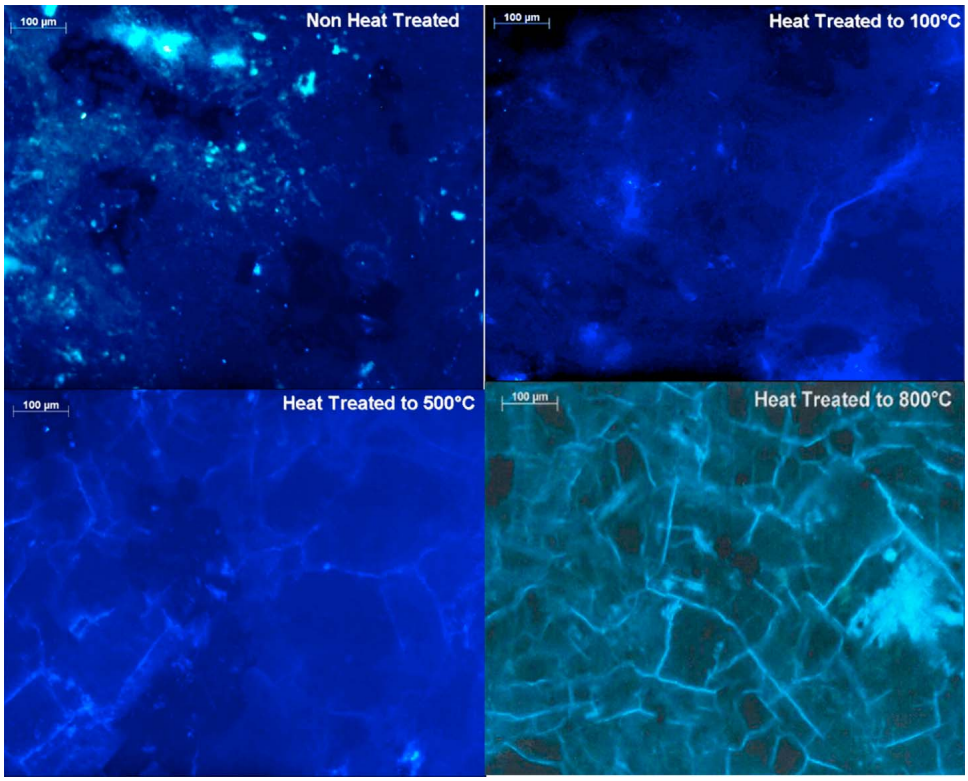

Figure 3. Photo-micrographs of (top left) the starting material (non-heat treated) and samples heat-treated to (top right) 100, (bottom left) 500 and (bottom right) 800°C. Long thin cracks can be distinguished from more open local pores caused by phenocryst alteration (light patches).

2005]. A mean pore fluid pressure, P_p, of 10 MPa was used subjecting the sample set to an effective pressure of 10 MPa, and our standard pressure difference across the sample was 1 MPa (i.e., 10.5 MPa upstream and 9.5 MPa downstream). However, in order to achieve steady state flow in an acceptable time frame (up to 15 days) for the very low permeability experiments it proved necessary to increase this pressure difference up to a maximum of 3 MPa. This introduces a potential source of systematic error from non-linear effects. To check its magnitude we made permeability measurements on the same intermediate-permeability sample using pressure differences of 1, 3 and 5 MPa. We found that differences in the measured permeability across the 3 values were less than 50%, i.e., small compared to the multiple orders of magnitude involved in the permeability range reported here.

4. Results

[10] The porosity of the starting material was determined using gas porosimetry to be 0.90%. Water permeability for the starting material was an astonishingly low 1.5×10^{-23} m^2, requiring fifteen days to make a single measurement. This is because the starting porosity occurs almost exclusively in altered feldspar micro-phenocrysts, which are sparsely but relatively evenly distributed through the rock volume (light patches in Figure 3, top left), and remain connected only through a few 'bottlenecks' due to the absence of connecting micro-fractures. Figures 3 (top right), 3 (bottom left), and 3 (bottom right) illustrate how the crack density, connectivity and aperture all increase systematically with respect to the ultimate temperature of the heat treatment. We confirmed that the induced crack damage was isotropic by such visual inspection and by azimuthal ultrasonic wave velocity measurements.

[11] The measured water permeability is plotted as a function of contemporaneously-measured porosity in the range 1–5% in Figure 4. The measured porosity represents the connected porosity and not the total porosity as applied in the percolation model of equation (1). This introduces a small but finite systematic error in the inferred model parameters that is discussed more fully along with the results below. In order to preclude further damage during sample preparation, fluid saturation and porosity measurements immediately before the permeability measurements was done under vacuum, leading to a low effective injection pressure of 1 bar (0.1 MPa). For the first two data points at the lowest permeability, this led to a measured fluid porosity during permeability measurements lower than the independently measured gas porosity of the starting material. Accordingly the first data point (corresponding to the starting material) was assigned a porosity of 0.9% and included in the regression, whereas the data point for permeability for the second sample is plotted merely for reference on Figure 4 as lying somewhere between the starting porosity and our lowest reliably-measured value, and not used in the regression.

[12] The optimal value for the threshold porosity Φ_c was found to be 0.85%, very close to the porosity of the starting material. The best fit curve for regression of $\log(K)$ v. $\log(\Phi - \Phi_c)$ for K_0 and n, given this value for Φ_c, is shown in Figure 4 along with its 95% confidence limits. These confidence limits are large compared to the systematic

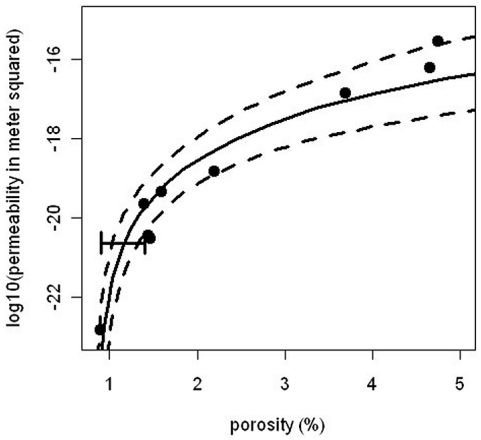

Figure 4. Comparison of the best fit (solid) curve and 95% confidence limits (dashed curves) to equation (1) with the data for the connected porosity and the bulk permeability. The horizontal bar indicates the possible range of porosity for the second data point.

uncertainties introduced by the method. The vertical range is on the order of 1–2 orders of magnitude in permeability, compared to a maximum error of 50% due to the high pressure drop discussed above. It is also unlikely the unconnected porosity at low porosity (Figure 3, top left) differs from the total porosity by more than the 10% or so difference in the confidence intervals in the horizontal direction at small porosity, though some systematic bias in the best fit parameters remains. With these caveats the best fit parameters are $n = 3.792 \pm 0.445$ and $\log K_0 = -18.776 \pm 0.248$, by least squares estimation. The regression coefficient $r^2 = 0.912$ for 9 data points, an F-statistic [*Dalgaard*, 2002] for the optimal regression of 72.51, and a P-value [*Weiss*, 1989] of 6.105×10^{-5}, all confirm the regression model is statistically significant well above the 95% confidence level. The results confirm the hypothesis of equation (1) at this level.

5. Discussion

[13] The measurements reported here are the bulk connected porosity and the steady-state macroscopic permeability at the sample scale, and can be used as effective parameters in modelling at higher scales, for example, in computer simulation of the integrity of sub-surface storage sites. At microscopic scales however, it is very unlikely that the flow is uniformly laminar. For the smallest porosity and permeability values reported here the effective aperture for local Poisueille flow may be less than 1 nanometre, where transport is instead very likely to occur by atomic-scale diffusion processes. For higher permeabilities there is likely to be a transition from such processes to Darcy flow with a scale-free viscosity. Further work is required to quantify the effect of such microscopic processes at very low porosities, and how they may affect the effective bulk parameters measured here.

[14] The high value of n inferred from Figure 4 is quantitatively most consistent with that predicted by the continuum percolation 'Swiss cheese' model [*Berkowitz and Balberg*, 1993], most likely due to its close resemblance to the actual fracture/pore network induced here (Figure 3). For different rock types we might expect equation (1) to hold, but with different values of the best fit parameters. We have also examined the simplest case of permeability in an isotropic material, in order to provide an important benchmark for the theory used and for later tests on anisotropic materials. In this general case we might expect the permeability to be a tensor rather than a scalar, either due to fabric or aligned microcracks in the starting material and/or to the effect of *in-situ* stresses associated with a given subsurface storage site. Systematic errors in the best fit results remain, though these are smaller than the statistical errors arising from a combination of experimental uncertainty and sample variability, shown at 95% confidence in Figure 4.

6. Conclusion

[15] Our new results confirm that the crack-induced permeability-porosity relation at very low permeability is similar to models proposed on the basis of transport near the percolation threshold, with a relatively high exponent n that can be explained by the microstructure of the crack/pore system. Hence, a modest change in total porosity from 1% to 5% or so results in a massive change in permeability of 7 orders of magnitude or more. The exponent n is similar to that for published data for rocks with much higher porosities, indicating the form of equation (1) may be universal. Having established this benchmark, further work is now required for the more general case of anisotropic materials and stress fields, and alternative barrier materials, notably the behaviour of tight shales and mud rocks that are a key element of current active proposals to develop carbon dioxide storage sites.

[16] **Acknowledgments.** O. Clint was supported by NERC grant GST/02/2307 as part of the 'Micro-to-Macro' thematic programme to carry out the experimental work. The material used in the experiments was donated by Donald Macrae of Kay's of Scotland, whose generosity and support we gratefully acknowledge. We thank Paul Glover and Joanne Fredrich for carrying out the external porosity measurements, Frank Schilling of GFZ, Potsdam, for providing the facilities that allowed the images of Figure 3 to be produced, Jean-Raynaud de Dreuzy, Philippe Davy and Ken Sorbie for useful discussions on percolation. The authors thank Teng-fong Wong and an anonymous reviewer for their insightful comments on the manuscript as submitted.

[17] The Editor thanks Teng-fong Wong and an anonymous reviewer for their assistance in evaluating this paper.

References

Benson, P. M., P. G. Meredith, E. S. Platzman, and R. E. White (2005), Pore fabric shape anisotropy in porous sandstones and its relation to elastic wave velocity and permeability anisotropy under hydrostatic pressure, *Int. J. Rock Mech. Min. Sci.*, *42*, 890–899, doi:10.1016/j.ijrmms.2005.05.003.

Berkowitz, B., and I. Balberg (1992), Percolation approach to the problem of hydraulic conductivity in porous media, *Transp. Porous Media*, *9*, 275–286, doi:10.1007/BF00611971.

Berkowitz, B., and I. Balberg (1993), Percolation theory and its application to groundwater hydrology, *Water Resour. Res.*, *29*, 775–794, doi:10.1029/92WR02707.

Bernabe, Y., W. F. Brace, and B. Evans (1982), Permeability, porosity and pore geometry of hot-pressed calcite, *Mech. Mater.*, *1*, 173–183, doi:10.1016/0167-6636(82)90010-2.

Brace, W. F., A. S. Orange, and T. R. Madden (1965), The effect of pressure on the electrical resistivity of water saturated crystalline rocks, *J. Geophys. Res.*, *70*, 5669–5678, doi:10.1029/JZ070i022p05669.

Dalgaard, P. (2002), *Introductory Statistics With R*, pp. 182–188, Springer, New York.

Darot, M., Y. Guèguen, and M. L. Baratin (1992), Permeability of thermally cracked Granite, *Geophys. Res. Lett.*, *19*, 869–872, doi:10.1029/92GL00579.

Feng, S., B. I. Halperin, and P. N. Shen (1987), Transport properties of continuum systems near the percolation threshold, *Phys. Rev. B*, *35*, 197–214, doi:10.1103/PhysRevB.35.197.

Fredrich, J. T., and T.-F. Wong (1986), Micromechanics of thermally induced cracking in three crustal rocks, *J. Geophys. Res.*, *91*, 12,743–12,764, doi:10.1029/JB091iB12p12743.

Glover, P. W. J., P. Baud, M. Darot, P. G. Meredith, M. Le Ravalec, S. Zoussi, and T. Reuschle (1995), Alpha/beta phase transition in quartz monitored using acoustic emissions, *Geophys. J. Int.*, *120*, 775–782, doi:10.1111/j.1365-246X.1995.tb01852.x.

Guèguen, Y., and J. Dienes (1989), Transport properties of rocks from statistics and percolation, *Math. Geol.*, *21*, 1–13, doi:10.1007/BF00897237.

Guèguen, Y., and V. Palciauskas (1994), *Introduction to the Physics of Rocks*, chap. 5 and 8, Princeton Univ. Press, Princeton, N. J.

Harrison, R. K., P. Stone, I. B. Cameron, R. W. Elliot, and R. R. Harding (1987), *Geology, Petrology and Geochemistry of Ailsa Craig, Ayrshire*, *Br. Geol. Surv. Rep.*, vol. 16, 29 pp., H.M.S.O., London.

Hopkin, M. (2007), Climate panel offers grounds for optimism, *Nature*, *447*, 120–121, doi:10.1038/447120a.

Intergovernmental Panel on Climate Change (2007), *Climate Change 2007: The Physical Science Basis. Contribution of Working Group I to the Fourth Assessment Report of the Intergovernmental Panel on Climate Change*, edited by S. Solomon et al., Cambridge Univ. Press, Cambridge, U. K.

Jones, C., and P. G. Meredith (1998), An experimental study of elastic wave propagation anisotropy and permeability anisotropy in an illitic shale, in *Proceedings of SPE/ISRM Rock Mechanics in Petroleum Engineering*, pp. 307–314, Soc. of Pet. Eng., Richardson, Tex.

Mavko, G., and A. Nur (1997), The effect of a percolation threshold in the Kozeny-Carman relation, *Geophysics*, *62*, 1480–1482, doi:10.1190/1.1444251.

Nara, Y., P. G. Meredith, T. Yoneda, and K. Kaneko (2011), Influence of macro-fractures and micro-fractures on permeability and elastic wave velocities in basalt at elevated pressure, *Tectonophysics*, *503*, 52–59, doi:10.1016/j.tecto.2010.09.027.

Stauffer, D., and A. Aharony (1994), *Introduction to Percolation Theory*, 2nd ed., Taylor and Francis, London.

Weiss, N. A. (1989), *Elementary Statistics*, 2nd ed., Addison and Wesley, New York.

Wong, P.-Z., J. Koplik, and J. P. Tomanic (1984), Conductivity and permeability of rocks, *Phys. Rev. B*, *30*(11), 6606–6614, doi:10.1103/PhysRevB.30.6606.

Zhang, S., M. S. Paterson, and S. F. Cox (1994), Porosity and permeability evolution during hot isostatic pressing of calcite aggregates, *J. Geophys. Res.*, *99*, 15,741–15,760, doi:10.1029/94JB00646.

Zhu, W. L., C. David, and T.-F. Wong (1995), Network modeling of permeability evolution during cementation and hot isostatic pressing, *J. Geophys. Res.*, *100*, 15,451–15,464, doi:10.1029/95JB00958.

O. C. Clint and P. G. Meredith, Department of Earth Sciences, University College London, Gower Street, London WC1E 6BT, UK.

L. Li and I. G. Main, School of Geosciences, University of Edinburgh, Grant Institute, West Mains Road, Edinburgh EH9 1NR, UK. (ian.main@ed.ac.uk)